

Photoelectron Angular Distributions of Rotationally Selected NO Rydberg States

J. Guo, A. Mank,* and J. W. Hepburn

Center for Molecular Beams and Laser Chemistry, University of Waterloo, Waterloo, Ontario, Canada N2L 3G1
(Received 17 October 1994)

The photoelectron angular distributions from autoionizing ns and nf Rydberg states of NO are presented. A striking dependence of the angular distribution on the rotational level in the excited Rydberg complex is observed: The sign of the asymmetry parameter β alternates for consecutive rotational levels. A multichannel quantum defect calculation shows qualitative agreement with the experimental results and indicates the role of predissociation in the decay of these Rydberg states.

PACS numbers: 33.20.Ni, 33.60.Cv, 33.80.Eh

In this Letter, we report photoelectron angular distributions that result from the excitation of single rotational levels of autoionizing Rydberg states of NO. This represents the first case where angle resolved photoelectron spectroscopy (ARPES) has been carried out following rotationally resolved single photon excitation. ARPES is an excellent tool for probing photoionization dynamics [1]. With incoherent light sources, hydrogen has been the only molecule for which a measure of rotational resolution has been achieved in ARPES [2]. Using resonantly enhanced multiphoton excitation (REMPI), photoionization from selected rotational levels of an intermediate state can be studied [3]. By direct ionization from high J levels in the $A^2\Sigma^+$ of NO, Zare and co-workers were able to resolve the rotational states of the NO^+ ion in time of flight (TOF) PES [4]. Using the properties of the intermediate state, they succeeded in giving a quantum mechanically complete description of the direct photoionization process. In this paper, attention will be focused on autoionization rather than direct ionization, and rotational state information will be obtained by high resolution excitation of Rydberg state resonances.

The Rydberg states of NO were first studied by Miescher [5] using absorption spectroscopy, and a long range interaction model was developed to describe the rotational structure of the nf Rydberg states [6,7]. Although the nf Rydberg electron generally has been regarded to exhibit little interaction with the ionic core, since the high centrifugal potential barrier prevents it from penetrating [5,6,8–10], the measured lifetimes of the rotational levels of several $nf(v=1)$ Rydberg states of NO [11], and the direct probe of predissociation products of nf Rydberg states of NO [12,13], indicate that autoionization and predissociation are competing decay channels, and that predissociation is actually faster than autoionization [13]. A recent study by Nussenzweig and Eyley [14] of the ns Rydberg states in NO suggests that autoionization is the dominant decay channel for these Rydberg states, although the s Rydberg electron should show much stronger interaction with the core, leading to enhanced predissociation.

For the study of photoionization from molecular ground states, the use of coherent vacuum ultraviolet (VUV) ra-

diation allows direct excitation of autoionizing Rydberg states, eliminating the requirement for an intermediate resonant state [15]. The combination of ARPES with coherent VUV allows one to measure the asymmetry parameter β for single rotational levels of autoionizing Rydberg states [16]. In this paper, we present photoelectron angular distributions (PADs) for autoionizing ns and nf Rydberg states in NO, obtained after single-photon excitation from the $J = \frac{1}{2}$ level of the ground state. In contrast with similar studies on HI [16], we observe a clear dependence of the angular distribution on the Rydberg rotational level, leading to a pattern of alternating signs for the asymmetry parameter β for consecutive rotational levels of the same Rydberg state. A calculation, using multichannel quantum defect theory (MQDT), is performed and shows generally good agreement with the experimental results. The differences between the experimental data and the theoretical calculation can be interpreted in terms of the interaction of the Rydberg states with the dissociative valence states.

The experimental setup has been described in detail elsewhere [17]. Linearly polarized, tunable, coherent VUV radiation with a bandwidth of 1 cm^{-1} was generated by resonantly enhanced four-wave difference-frequency mixing in a krypton jet. The polarization direction of VUV radiation was controlled by rotating the polarization direction of the input beams with a Fresnel rhomb half-wave retarder. A polarization analyzer [18] was placed behind the ionization volume and used to monitor the polarization of the VUV radiation. The skimmed supersonic beam was prepared with 5% NO seeded in neon yielding a rotational temperature of less than 3 K, giving a population of 95% in the $J = \frac{1}{2}$ rotational level of the $^2\Pi_{1/2}$ spin-orbit component of the NO ground state. Photoions and photoelectrons were analyzed by a TOF spectrometer perpendicular to both the VUV beam and the molecular beam.

The experimental results for the rotational structure of the autoionizing $10f(v=2)$ Rydberg state of NO are shown in Fig. 1. The angular momentum coupling of the nf Rydberg states follows Hund's case (d); therefore, the rotational levels are labeled by N^+ , the angular

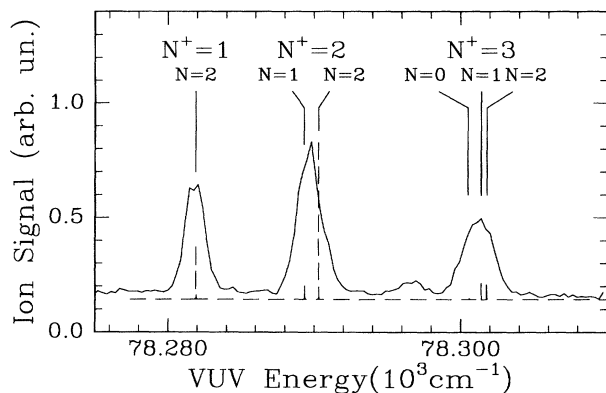


FIG. 1. The photoionization efficiency spectrum of the $10f(v=2)$ Rydberg state. The experimental results are given by a solid line and the dashed line is the result of an MQDT calculation. The rotational levels are labeled by N^+ , the rotational quantum number of the ionic core and N , the total angular momentum.

momentum of the ionic core, and by N , the total angular momentum of the Rydberg state. Whereas the levels of N^+ are clearly resolved, the subrotational levels N have not been resolved. The $10f(v=2)$ Rydberg state decays via vibrational autoionization preferentially into the $v^+ = 1$ continuum [19]. The corresponding PADs for this autoionization channel are shown in Fig. 2. The asymmetry parameter β is derived by a fit of the analytical form

$$\frac{d\sigma}{d\Omega} = \frac{\sigma}{4\pi} \left[1 + \beta \left(\frac{3}{2} \cos^2\theta - \frac{1}{2} \right) \right].$$

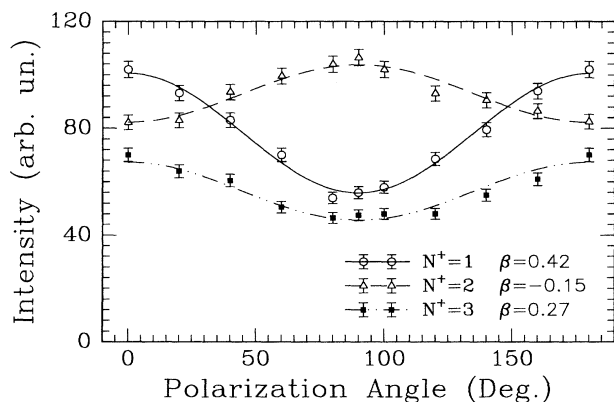


FIG. 2. Experimental results for the photoelectron angular distribution at the peaks of the rotational lines for the $10f(v=2)$ Rydberg state. The results are denoted by symbols with error bars, giving the statistical uncertainty. The lines are the result of a fit by the expected analytical form of the angular distribution, yielding the asymmetry parameter β denoted in the figure.

TABLE I. Experimental angular distribution asymmetry parameter β for the nf Rydberg states. Except when noted, the final state is NO^+ , $X^1\Sigma^+$, $v^+ = 1$. The typical error is ± 0.1 . For $N^+ = 2$ and $N^+ = 3$ the asymmetry parameter β is averaged over the subrotational levels N , except where noted.

	$N^+ = 1$	$N^+ = 2$	$N^+ = 3$
$10f(v=1)^a$	0.43	0.25	0.35
$11f(v=1)^a$	0.69	0.36	0.27
$5f(v=3)$	0.34	0.37 ($N=1$) 0.37 ($N=2$)	0.43 ($N=2$)
$8f(v=2)$	0.32	-0.26 ($N=1$)	0.44
$9f(v=2)$	0.54	-0.07	0.27
$10f(v=2)$	0.42	-0.15	0.27
$11f(v=2)$	0.38	-0.13	0.27
$13f(v=2)$	0.21	-0.12	0.25
$8f(v=3)^b$	0.38	-0.13 ($N=1$) 0.13 ($N=2$)	0.39

^aThe final state is NO^+ , $^1\Sigma^+$, $v^+ = 0$.

^bThe final state is NO^+ , $^1\Sigma^+$, $v^+ = 2$.

The experimental results for the asymmetry parameter β are listed in Tables I and II, respectively. In general, they show a similar pattern of alternation with the rotational level of the Rydberg complex. This pattern is the same for all the $ns\sigma$ Rydberg states investigated, whereas for the nf Rydberg states there are some interesting differences. All the $v=1$ and $v=2$ resonances of nf Rydberg states studied decay through a $\Delta v = -1$ process [19], but the $v=1$ resonances do not show the alternation in the sign of the asymmetry parameter. The $5f(v=3)$ resonance cannot decay through a $\Delta v = -1$ process, and does not show the alternation in sign either. For the $8f(v=3)$ resonance, it is possible to resolve the subrotational structure of $N^+ = 2$, and the two levels show different asymmetries.

To understand these results, an MQDT calculation has been performed for the nf Rydberg states. The method of Greene and Jungen [20] was used to calculate the PADs for the nf Rydberg states. It was assumed

TABLE II. Experimental angular distribution asymmetry parameter β for the ns Rydberg states. Except when noted, the final state is NO^+ , $X^1\Sigma^+$, $v^+ = 1$. The typical error is ± 0.12 .

	$N = 0$	$N = 1$	$N = 2$
$11s\sigma(v=1)^a$	0.13	-0.01	0.52
$7s\sigma(v=2)^a$	0.37	-0.09	0.52
$9s\sigma(v=2)$	0.26	0.01	0.33
$10s\sigma(v=2)$	0.08	-0.17	0.25
$11s\sigma(v=2)$	0.26	-0.15	0.42
$7s\sigma(v=3)$	0.17	-0.08	0.35
$12s\sigma(v=2)$	0.48	-0.03	0.40

^aThe final state is NO^+ , $^1\Sigma^+$, $v^+ = 0$.

that the angular momentum of the Rydberg electron is preserved during autoionization, which is the case for pure vibrational autoionization [20], and neither the spin of the photoelectrons nor predissociation is included in the MQDT calculation. The electron in the ground state is considered to have d character, and the transition dipole matrix elements from the ground state to $f\sigma, f\pi, f\delta$ are set to 1 [21]. The quantum defects and their R dependences have been obtained by fitting to published spectroscopic data [19]. According to Fano and Dill [22,23] the transferred angular momentum J_t is given by

$$J_t = J_\gamma - l = J^+ - N'',$$

where J_γ is the photon angular momentum ($J_\gamma = 1$), J^+ is the angular momentum of the final state of the ion, and N'' is the rotational angular momentum in the ground state, excluding spin. For each allowed value of J_t , there is a defined asymmetry parameter $\beta(J_t)$. The total angular distribution asymmetry parameter β as follows [23]

$$\beta = \frac{\sum_{J_t} \sigma(J_t) \beta(J_t)}{\sum_{J_t} \sigma(J_t)},$$

where $\sigma(J_t)$ is the cross section for J_t . Since l equals 3, J_t can be 2, 3, and 4, and the three β parameters are [22,23]

$$\beta(J_t = 2) = \frac{4}{3}, \quad \beta(J_t = 3) = -1, \quad \beta(J_t = 4) = \frac{1}{3}.$$

The cross section $\sigma(J_t)$ can be expressed as

$$\sigma(J_t) = \pi \lambda^2 \frac{2J_t + 1}{2N'' + 1} |\langle v^+ J^+ | \bar{S}(J_t) | v'' N'' \rangle|^2,$$

$$\langle v^+ J^+ | \bar{S}(J_t) | v'' N'' \rangle = \sum_N (-1)^{N-N''+1} (2N + 1) \times \begin{Bmatrix} 3 & 1 & J_t \\ N'' & J^+ & N \end{Bmatrix} \langle v^+ J^+ | \bar{S}(N) | v'' N'' \rangle,$$

where λ is the wavelength of the incident radiation (divided by 2π) and the $\langle v^+ J^+ | \bar{S}(N) | v'' N'' \rangle$ term is obtained from the MQDT calculation. Typical results of the calculation are listed in Table III.

The autoionization of the nf Rydberg states can be classified into two types according to whether the $\Delta v =$

-1 autoionization channel is open or closed. When the $\Delta v = -1$ channel is open, it becomes the dominant autoionization channel [19]. Since the photoelectrons are mainly produced by rovibrational autoionization, there is good agreement between calculation and experiment for the $8f(v = 3)$ Rydberg complex, where the resonances of $N^+ = 2, N = 1$, and $N^+ = 2, N = 2$ are separated. When the resonances are not resolved, as is the case for the $10f(v = 2)$ Rydberg state given in Fig. 1, the measured PADs have contributions from both subrotational levels and depend strongly on their relative intensities. The MQDT calculation agrees with the experimental results for the $nf(v = 1)$ resonances, whereas for the $nf(v = 2)$ Rydberg states, the experimental results differ. The discrepancy can be explained by looking at the relative intensities of the subrotational levels. These levels have been resolved for the $8f(v = 2)$ resonance. If the experimentally observed branching ratio for $8f(v = 2)$ [19] is used in the calculation of the β parameter of the other $nf(v = 2)$ states, the result is $\beta = -0.21$, which agrees with the experimental data. One possible explanation is that the predissociation changes the relative intensities of the subrotational levels. The difference in the branching ratio for the $nf(v = 1)$ to $nf(v = 2)$ resonances may be due to different Franck-Condon overlap between the Rydberg states and the predissociative valence states.

When the $\Delta v = -1$ autoionization channel is closed, as in the $5f(v = 3)$ resonance, the vibrational autoionization rate is greatly reduced and autoionization via the dissociative states becomes the dominant mechanism [24]. From the PADs of the $5f(v = 3)$ resonance it can be seen that autoionization via the dissociative states yields an asymmetry parameter β of ~ 0.4 . This result cannot be explained by our MQDT calculation, which assumed that the l of the photoelectron has the same value as the Rydberg electron, indicating substantial l mixing in the autoionization channel.

From the nf Rydberg series, it is clearly seen that the predissociative valence states interact with the nf Rydberg states and affect the PAD either indirectly, by changing the relative intensities of the rotational sublevels, or directly, by changing the dynamics of the autoionization process. Although, in principle, predissociation can be included in the MQDT calculations, lack of knowledge about the nature of the valence states and electronic coupling involved in the predissociation prevent such calculations at the present time.

The PADs of the $ns\sigma$ Rydberg states show a more consistent alternation of the asymmetry parameter β , even in the $\Delta v = -2$ channel. Although the $ns\sigma$ Rydberg states are strongly mixed with the $nd\sigma$ Rydberg states and the predissociation is considered to be important, the pattern of the PADs given in Table II can be explained by assuming rovibrational autoionization [19], which strongly suggests that the predissociation in the $ns\sigma$ Rydberg states is

TABLE III. Results of an MQDT calculation for the angular distribution asymmetry parameter β . The theoretical results are convoluted with the experimental bandwidth of 0.8 cm^{-1} . The convolution leads to an averaging of the N levels for $N^+ = 2$ for the $10f$ states. The autoionization proceeds via the $\Delta v = -1$ channel, except for the $5f(v = 3)$ Rydberg state, where it is $\Delta v = -2$. The β parameter for the $N^+ = 3$ are mixtures of the subrotational levels N , except for $5f(v = 3)$, which is for $N = 2$.

	$N^+ = 1$ $N = 2$	$N^+ = 2$ $N = 1$ $N = 2$	$N^+ = 3$
$10f(v = 1)$	0.64	0.16	0.25
$5f(v = 3)$	0.35	-0.21 0.18	0.03
$10f(v = 2)$	0.63	0.16	0.23
$8f(v = 3)$	0.62	-0.36 0.18	0.40

considerably weaker than autoionization. By comparing the linewidth of $ns(v = 1)$ and $nf(v = 1)$ Rydberg states [11,14], it can be concluded that the predissociation of the ns levels is weaker than that of the nf levels in NO Rydberg states.

Although the MQDT calculations provide a basis for a quantitative comparison with the data, the reason for the alternation in the sign of the asymmetry parameter is quite straightforward. The key to observing this effect is rotational resolution in the excitation step, and the alternation effect is a result of vibrational autoionization, where one expects the l quantum number of the Rydberg electron to be unchanged by autoionization, creating a well-defined outgoing wave. This clear selection of angular momentum quantum numbers gives rise to the alternation in β with N^+ , as can be seen by the equations given earlier.

The MQDT calculations reported in this paper are based on earlier work carried out in collaboration with Ch. Jungen. A more detailed presentation of this work will be given in a future paper [19]. The authors would also like to acknowledge helpful discussions with H. Lefebvre-Brion and G. Raseev. J.G. would like to thank R.J. LeRoy and J.D.D. Martin for their help in the MQDT calculation. Financial support by the Natural Sciences and Engineering Research Council (NSERC) and the Network of Centers of Excellence in Molecular and Interfacial Dynamics (CEMAID), administered by NSERC is acknowledged.

*Present address: Department of Chemistry, University of Toronto, 80 St. George Street, Toronto, Ontario, Canada M5S 1A1.

- [1] J.L. Dehmer, Dan Dill, and A.C. Parr, in *Photophysics and Photochemistry in the Vacuum Ultraviolet*, edited by S.P. McGlynn, G.L. Findley, and R.H. Huebner (D. Reidel Publishing Company, Holland, 1985).
- [2] A. Niehaus and M.W. Ruf, *Chem. Phys. Lett.* **11**, 55 (1971).
- [3] S.T. Pratt, P.M. Dehmer, and J.L. Dehmer, in *Advances in Multi-Photon Processes and Spectroscopy*, edited by S.H. Lin (World Scientific, Singapore, 1984), Vol. 4.
- [4] K.L. Reid, D.J. Leahy, and R.N. Zare, *Phys. Rev. Lett.* **68**, 3527 (1992); D.J. Leahy, K.L. Reid, H. Park, and R.N. Zare, *J. Chem. Phys.* **97**, 4948 (1992).
- [5] E. Miescher, *Can. J. Phys.* **54**, 2074 (1976), and references therein.
- [6] Ch. Jungen and E. Miescher, *Can. J. Phys.* **47**, 1769 (1969).
- [7] E.E. Eyler and F.M. Pipkin, *Phys. Rev. A* **27**, 2462 (1983); E.E. Eyler, *ibid.* **34**, 2881 (1986).
- [8] E.F. McCormack, S.T. Pratt, J.L. Dehmer, and P.M. Dehmer, *Phys. Rev. A* **44**, 3007 (1988).
- [9] Ch. Jungen, I. Dabrowski, G. Herzberg, and M. Vervloet, *J. Chem. Phys.* **93**, 2289 (1990); G. Herzberg and Ch. Jungen, *ibid.* **77**, 5876 (1982).
- [10] M. Vervloet, A.L. Roche, and Ch. Jungen, *Phys. Rev. A* **38**, 5489 (1988).
- [11] E.E. Eyler, W.A. Chupka, S.D. Colson, and D.T. Biernacki, *Chem. Phys. Lett.* **119**, 177 (1985); D. Therese, S.D. Colson, and E.E. Eyler, *J. Chem. Phys.* **89**, 2599 (1988).
- [12] A. Fujii and N. Morita, *Chem. Phys. Lett.* **182**, 304 (1991).
- [13] A. Fujii and N. Morita, *J. Chem. Phys.* **97**, 327 (1992).
- [14] A. Nussenzeig and E.E. Eyler, *J. Chem. Phys.* **101**, 4617 (1994).
- [15] J.W. Hepburn, in *Vacuum Ultraviolet Photoionization and Photodissociation of Molecules and Clusters*, edited by C.Y. Ng (World Scientific, Singapore, 1991); J.W. Hepburn, in "Laser Techniques in Chemistry," edited by A. Myers and T.R. Rizzo (John Wiley & Sons, New York, to be published).
- [16] A. Mank *et al.*, *J. Electron Spectrosc.* **52**, 661 (1990); A. Mank *et al.*, *Z. Phys. D* **29**, 275 (1994).
- [17] W. Kong *et al.*, *J. Chem. Phys.* **99**, 3195 (1993); W. Kong, D. Rodgers, and J.W. Hepburn, *ibid.* **99**, 8571 (1993).
- [18] K. Rabinovitch, L.R. Canfield, and R.P. Madden, *Appl. Optics* **4**, 1005 (1965).
- [19] J. Guo, A. Mank, Ch. Jungen, and J.W. Hepburn (to be published).
- [20] C.H. Greene and Ch. Jungen, *Adv. At. Mol. Phys.* **21**, 51 (1986).
- [21] K.P. Huber *et al.*, *J. Chem. Phys.* **100**, 7957 (1994).
- [22] U. Fano and D. Dill, *Phys. Rev. A* **6**, 185 (1972).
- [23] D. Dill, *Phys. Rev. A* **7**, 1976 (1973).
- [24] A. Giusti-Suzor and Ch. Jungen, *J. Chem. Phys.* **80**, 986 (1984); Y. Achiba and K. Kimura, *Chem. Phys.* **129**, 11 (1988).